

Investigating Two Scales of In-Line Multi-Jets Ozone Contactors

Mahad S. Baawain¹, Mohamed Gamal El-Din², Daniel W. Smith² and Angelo Mazzei³

1. Department of Civil & Architectural Engineering, Sultan Qaboos University, Muscat, Oman
2. Department of Civil & Environmental Engineering, University of Alberta, Edmonton, Canada
3. Mazzei Injector Corporation, Bakersfield, CA

Abstract

This study investigates the mixing and ozone mass transfer characteristics of two scales of in-line multi-jets ozone contactors. The hydrodynamic characteristics of the two contactors were studied by using a laser flow map particle image velocimetry coupled with planar laser induced fluorescence (PIV/PLIF). All measurements were conducted under total liquid flow rate of about 10 L/s (for 0.10 m diameter contactor) and 5.5 L/s (for 0.075 m diameter contactor) with gas flow rate ranging from 0.05 to 0.4 L/s (for 0.10 m diameter contactor) and 0.03 to 0.24 L/s (for 0.075 m diameter contactor). Side injectors (opposing and alternating modes) were used to introduce the gas to the contactors. It was found that for the same number of jets (i.e. same gas flow rate) the liquid dispersion (D_L) was higher when alternating jets were used. Higher ozone mass transfer rates were observed when using opposing jet compared to the same number of alternating jets.

Key words: Ozone; hydrodynamics; mixing; mass transfer; dispersion coefficient; laser; particle image velocimetry; planar laser induced fluorescence.

Introduction

Effective reactor's design requires information, knowledge, and experience from different areas including chemical kinetics, fluid mechanics, and mass transfer (Levenspiel, 1999). Consequently, there is high complexity associated with the accuracy in estimating parameters needed for each area mentioned above. Therefore, empirical and semi-empirical relationships are used in designing such reactors. Unfortunately, these relationships are not reliable and/or valid over a wide range of applications encountered in practice (Joshi, 2002). Furthermore, recent concerns resulted from the existence of micro-pollutants in drinking water supplies (Petrovic et al., 2003) urge the need for accurate design of advanced water and wastewater treatment reactors. Thus, a proper design procedure is needed in order to reduce the prevailing empiricism associated with conventional water treatment reactors. Joshi and Ranade (2003) recommended the following procedure: (1) identify desired fluid dynamic characteristics by understanding

process requirements, (2) develop possible reactor configurations/operating protocols to attain the preferred fluid dynamic characteristics, (3) develop quantitative relationships between the reactor configuration and the observed performance, and (4) optimize the final reactor design.

The use of non-intrusive (*i.e.*, no direct interaction with the flow field) measurement methods such as laser measurement systems can offer accurate hydrodynamic characteristics of certain reactors. These laser systems are directional sensitive in addition to their accurate and high resolution measurements (Albrecht et al., 2002). Examples of laser systems used to evaluate reactors' hydrodynamic characteristics include: laser Doppler anemometer (LDA), particle dynamics analyzer (PDA), particle image velocimetry (PIV), and planer laser induced fluorescence (PLIF) (Albrecht et al., 2002; Atkinson et al., 2000). Both LDA and PDA systems are used to provide the flow velocity at one point in a flow field (PDA can also supply a simultaneous measurement of particles' size) (Durst et al., 1997). The PIV system can provide simultaneous planar measurements of flow velocities by measuring the displacement of seeded particles over relatively short time intervals (Atkinson et al., 2000; Bernard and Wallace, 2002, Raffel et al., 1998). The PLIF system is utilized to obtain a scalar concentration field in water by introducing a fluorescent dye as a passive scalar in the flow. The dye absorbs incident light, during the illuminating process of the laser, at a certain wavelength and re-emits it at a different wavelength with an intensity that is proportional to the dye concentration at the measuring point (Bernard and Wallace, 2002).

The objectives of this study are: (1) characterize the hydrodynamics of two scales of in-line multi-jets ozone contactor utilizing PIV/PLIF laser measurement techniques, (2) investigate the mass transfer efficiency of the contactors, and (3) optimize the systems operating conditions.

Experimental

Two pilot-scales in-line multi-jets ozone contactors were used in this study. Both contactors were made of clear acrylic glass and had 2000 mm lengths. The small size reactor had an inner diameter of 75 mm while the larger reactor's diameter was 100 mm. The experimental set up used in the hydrodynamic investigation for each contactor in this study consisted of a laser source, a charge coupled device (CCD) camera, and processing units (Figure 1). Outer square jackets of 120 mm sides for the smaller contactor and 150 mm for the larger contactor were used to reduce the reflection effect of the laser from the contactor curved surface. Each jacket had 1500 mm length. The water was introduced to the contactors from a 2000 L tank through a main stream and two side streams. The side stream lines had multi jets (Mazzei[®] venturi injectors; model 484 with N-7 nozzle for the smaller contactor and model 584 with N-8 nozzle for the larger contactor). These jets introduce the gas to the system in either injection or suction modes. The end of the contactors had two outlets to allow for recycling or draining of the water passing through the systems.

An Nd:Yag dual cavity laser with 150 mJ power level was utilized in this study for both the PIV and PLIF experiments. The emitted wavelength of the applied Nd:Yag laser was 532 nm with a pulse duration of 10 ns. The period between pulses was 1000 μ s during PIV measurements and 100 μ s during PLIF measurements with a maximum repetition rate of 8.0 Hz. The CCD cameras

were configured to use double frames for the PIV runs (velocity measurements) and a single frame for PLIF run (concentration measurements). A FlowMap System Hub[®] produced by Dantec Dynamics was utilized to transfer the data to a PC where FlowMap Software[®] was used for data analysis.

The experimental conditions conducted in this study for both PLIF and PIV measurements applied on the smaller contactor are summarized in Table 1. The experimental conditions applied on the larger contactor can be obtained from Baawain et al. (2007). The PLIF system was first calibrated by measuring the intensity of 5 different concentrations of Rhodamine 6G (Rh6G) solutions ranging from zero to 500 $\mu\text{g/L}$ for the larger contactor and from zero to 150 $\mu\text{g/L}$ for the smaller contactor. The calibration process for each contactor was conducted at a power level ranging from 50 to 150 mJ. The concentration versus the intensity were plotted (for each contactor) to determine the most appropriate calibration curve for the study. The calibration curves obtained for the 150 mJ power gave the highest correlation coefficient (0.85 and 0.95 for the larger and smaller contactors, respectively). Therefore, this power level was used for the PLIF measurements conducted for both contactors. After reaching a steady state flow condition for both contactors, a continuous injection of a 12.5 mg/L, for larger contactor, and 5.5 mg/L, for the smaller contactor, of the Rh6G tracer at about 0.063 L/s (yield about 80 $\mu\text{g/L}$ average concentration when mixed with the total liquid flow rates of the contactors) was introduced to the system through an injection point at the entrance of the contactor as shown in Figure 1. The PLIF procedure of image capturing covered about 5 times the detention time required for the tracer to pass through the system under each operating condition. (Duplicate measurements were taken to reduce uncertainty associated with the measurements.)

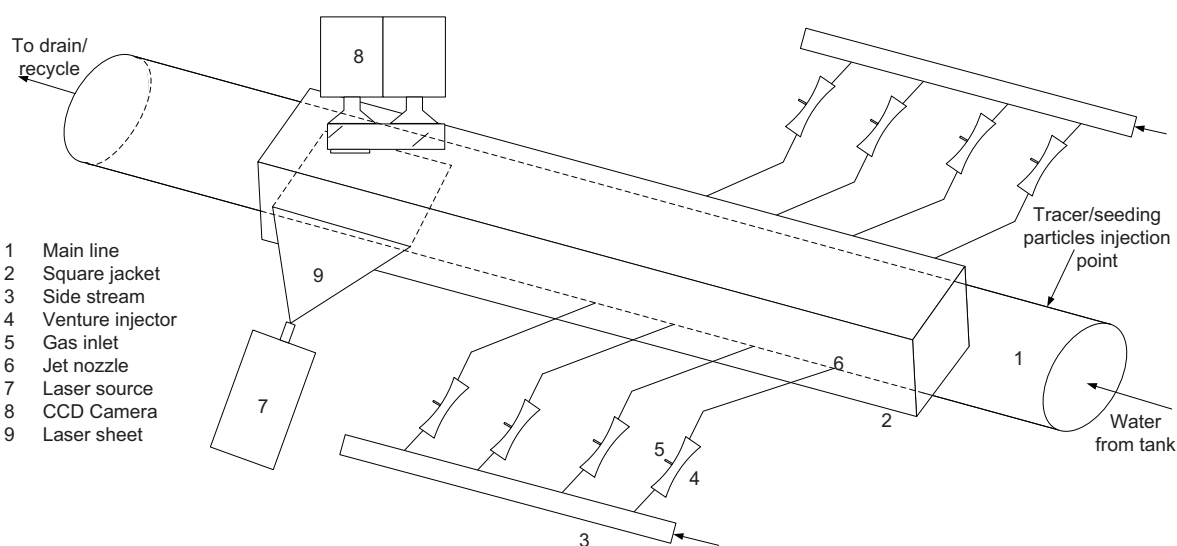


Figure 1. Experimental setup [adopted from Baawain et al. (2007)].

The PIV measurements were taken using two CCD cameras with a double-frame mode for measuring the velocity of both phases (liquid and gas) simultaneously utilizing special filters. Melamine-formaldehyde (MF) spheres, coated with Rhodium B (RhB), were used as seeding particles during the liquid velocity measurements while gas bubbles represented the seeding

particles used for the gas velocity measurements. Gas flow rate (Q_G) for the smaller contactor ranged from 0.03 L/s (for one jet) to 0.24 L/s (for eight jets) which correspond to a range of gas to liquid ratio of 0.5% to 4%. The PIV process of image capturing was taken in duplicate measurements.

A gas mass transfer analysis was also conducted to investigate the performance of the contactors under the studied operating conditions (Table 1). The experimental setup consisted of the pilot-scale multi-jets ozone contactors and two dissolved oxygen (DO) probes that were placed in the contactor (one upstream of the jets and one downstream of the two phase jets) to obtain DO measurements directly. The change in DO concentrations was monitored with time under each operating condition to determine the overall mass transfer coefficient of oxygen ($k_L a - O_2$, s^{-1}). Then, the obtained $k_L a - O_2$ was used to determine the overall mass transfer coefficient of ozone ($k_L a - O_3$, s^{-1}) by applying the following relationship which was introduced by Danckwert (1970) and validated by Sherwood et al. (1975):

$$[1] \quad \frac{k_L a - O_3}{k_L a - O_2} = \sqrt{\frac{D_{O_3}}{D_{O_2}}}$$

where, D_{O_3} and D_{O_2} are the molecular diffusivities of ozone and oxygen gases, respectively, in water (1.74×10^{-9} and 2.50×10^{-9} m^2/s , respectively). The ozone-based $k_L a - O_3$ values were obtained at 20 °C by using the following relationship (Roustan et al., 1996):

$$[2] \quad (k_L a - O_3)_{20} = (k_L a - O_3)_T 1.024^{20-T}$$

where, T is water temperature in the contactor (°C). Water temperature (T) ranged from 10 to 17 °C.

Table 1. Summary of the operating conditions during PIV, PLIF and mass transfer experiments for the 0.075 m diameter contactor.

Experiment number	# of jets	Jet alignment*	Liquid flowrate, Q_L (L/s)	Gas flowrate, Q_G (L/s)
1	1	-	5.5	0.03
2	2	O	5.5	0.06
3	2	A	5.5	0.06
4	3	A	5.5	0.09
5	4	O	5.5	0.12
6	4	A	5.5	0.12
7	5	A	5.5	0.15
8	6	O	5.5	0.18
9	6	A	5.5	0.18
10	7	A	5.5	0.21
11	8	O	5.5	0.24
12	8	A	5.5	0.24

* O = opposing; A = alternating

Results and Discussion

Reactor's Hydrodynamics

All images captured during the PLIF experiments were transformed into 2D concentration fields through the obtained calibration relation using the FlowMap software. A re-sampling of the concentration fields yielded colored contour maps that show the concentration distribution of the tracer along the cross-section of the contactor and parallel to the flow direction. A typical colored contour map representing the concentration distribution at different sampling times is shown in Figure 2. The figure shows contour maps for 4 opposing and 4 alternating jets with Q_L of 5.5 L/s and Q_G of 0.09 L/s. It can be seen that segments of higher tracer concentration pass through the contactor with 4 alternating jets relatively faster than 4 opposing jets. This implies a higher axial dispersion in the case of alternating jets compared to the opposing jets case. Furthermore, a relatively lower cross-sectional mixing can be observed in the case of the alternating jets compared with the opposing ones.

Samples of velocity vectors obtained from the PIV measurement at the mixing zone (outlet of the jets) are shown in Figure 3 as indicated previously by Baawain et al. (2007) (0.10 m diameter contactor). A better cross-sectional mixing can be observed in both liquid and gas phases when opposing jets are used. Moreover, the axial velocity in both phases (liquid and gas) are relatively higher when alternating jets are used which explains their higher axial dispersion observed in Figure 2. Results obtained from the PIV system for the smaller contactor were very similar to the larger contactor.

Baawain et al. (2007) have demonstrated the method of evaluating the hydrodynamics of the contactor using PLIF results by obtaining step response curves (F-curves) at any position of interest. The F-curves represent the dimensionless concentration (F) as a function of the time. A typical F curve obtained from the PLIF experiments at the centre of the images captured for $Q_L = 10$ L/s and $Q_G = 0.2$ L/s is shown in Figure 4a (for the 0.10 m diameter contactor). In order to obtain the dispersion number (inverse of Peclet number) under each operating condition, the probability plot method was employed as shown in Figure 4b. The standard deviation (σ , s) was obtained by using the following equation:

$$[3] \quad \sigma = \frac{t_{84\%} - t_{16\%}}{2}$$

where $t_{84\%}$ and $t_{16\%}$ are the times corresponding to 84% and 16%, respectively, of the tracer passing through the contactor's outlet. Then the dimensionless standard deviation was determined as follows:

$$[4] \quad \sigma_\theta = \frac{\sigma}{\tau}$$

where τ is the theoretical detention time of the contactor. The dispersion number can then be computed as:

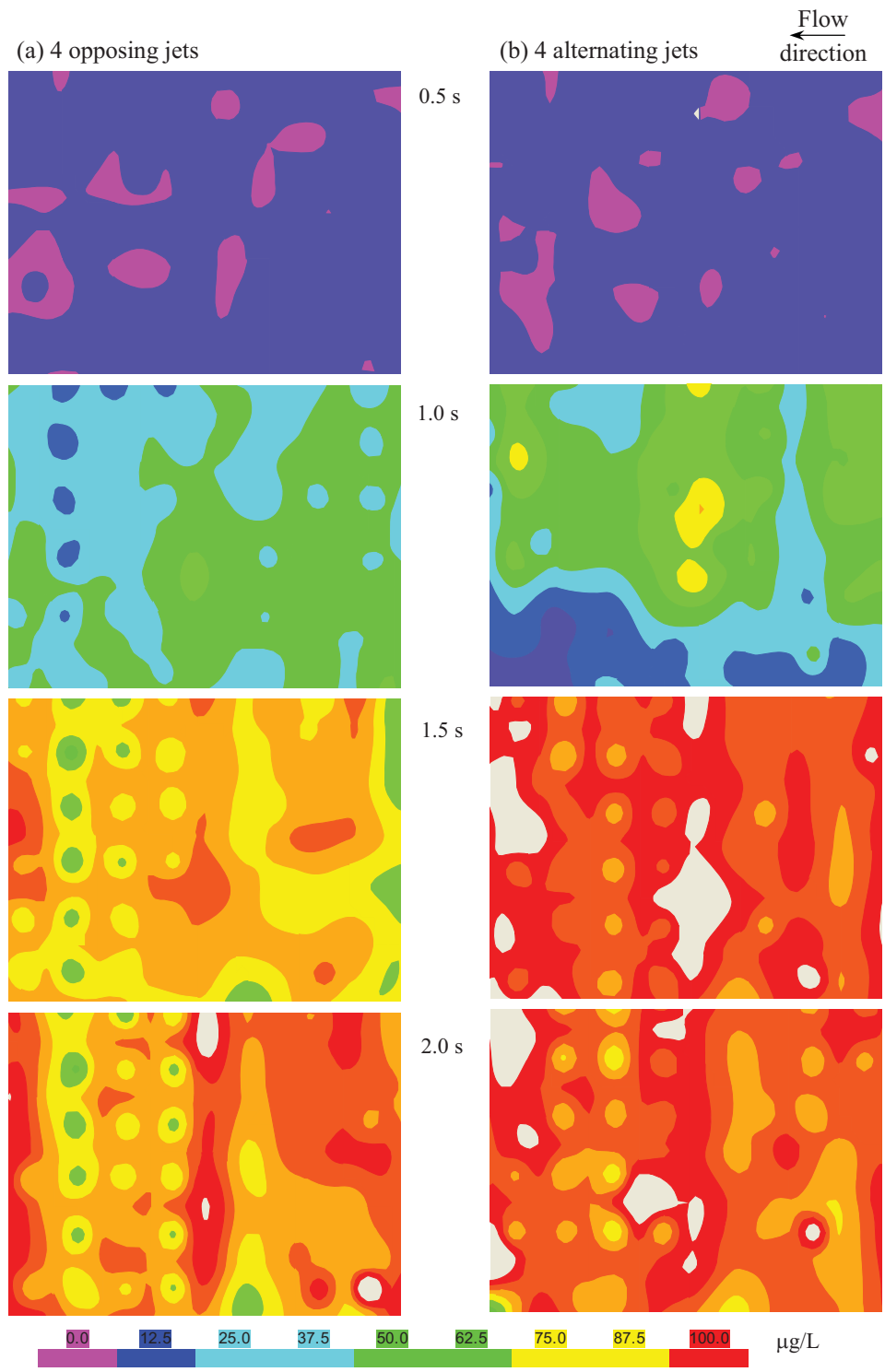


Figure 2. Tracer concentration for 4 jets (opposing and alternating).

$$[5] \quad \frac{D_L}{uL} = \frac{\sigma_\theta^2}{2}$$

where, D_L/uL is the dispersion number, D_L is the axial liquid dispersion coefficient (m^2/s), u is the liquid average axial velocity (m/s), and L is the contactor length (m). Obtained results showed that the dispersion number increases as the number of two-phase jets increases, which can be the increased amount of gas introduced to system. Moreover, for the same number of jets, it was noted that the dispersion number is higher in the case of alternating jets which might be due to the lower cross-sectional mixing posed by the alternating jets compared to the opposing ones.

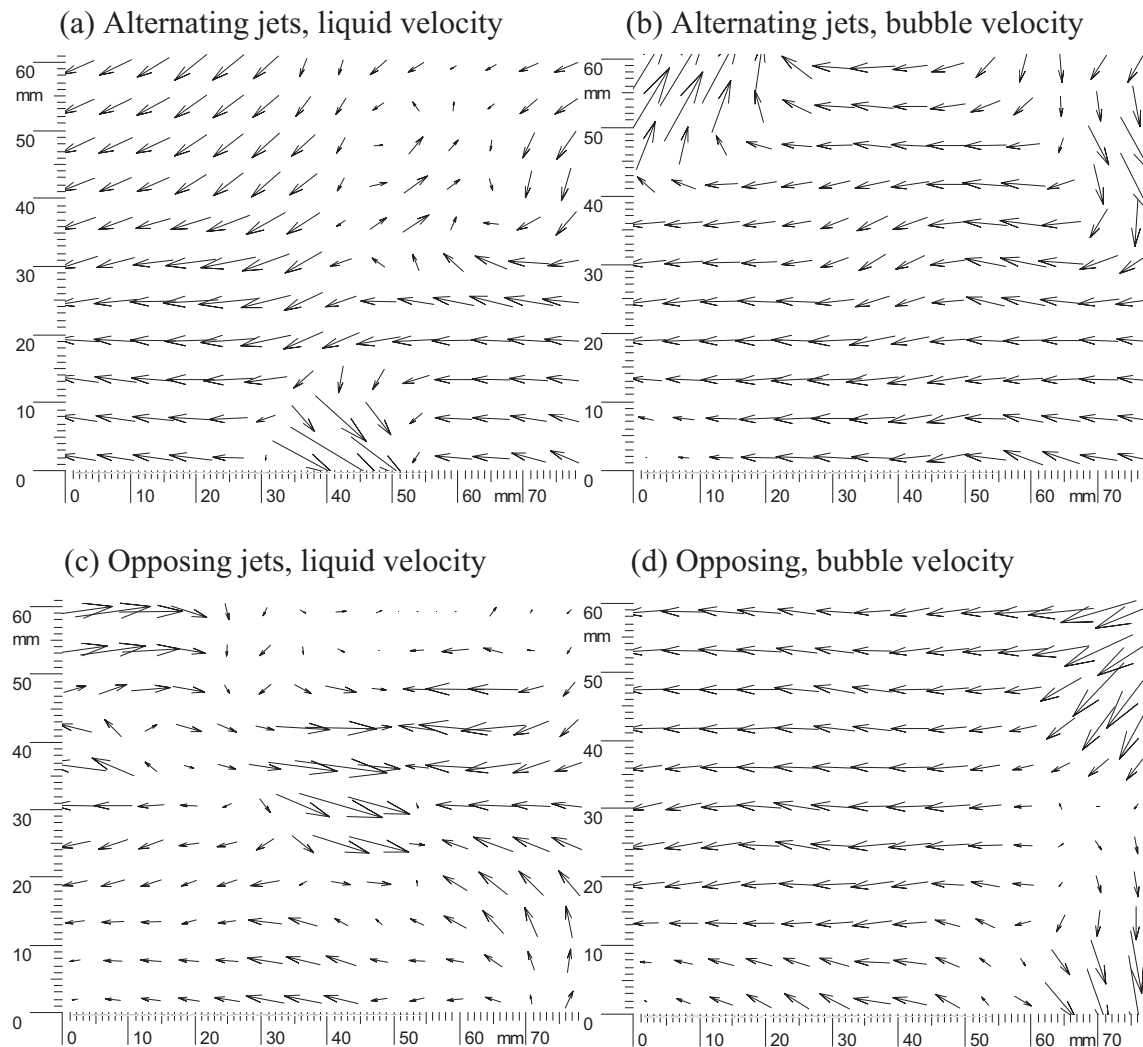


Figure 3. Velocity vectors for alternating and opposing jets at inlet zone (scale: 5 mm = 1 m/s) [adopted from Baawain et al. (2007)].

Gas Mass Transfer

The following empirical relationship, proposed by Deckwer *et al.* (1974), was used to show the effect of u_G on k_La :

$$[6] \quad k_La = \alpha u_G^\beta$$

where: α and β are empirical constants that are obtained through a non-linear regression analysis. Figure 5 shows the experimental results of the ozone based k_La for both ozone contactors under different u_G values. It can be seen that as the number of two-phase jets increases (i.e. gas flow rate increases), the value of k_La increases. Moreover, using opposing jets in both contactors yielded higher k_La values at the same u_G value, which can be related to the lower D_L values of the opposing jets discussed earlier. Furthermore, the k_La values obtained for the 0.075 m diameter contactors were about 30% lower than those obtained for the 0.10 m diameter contactor. This can be related to the lower cross-sectional volume available mass transfer in the smaller contactor compared to the larger one.

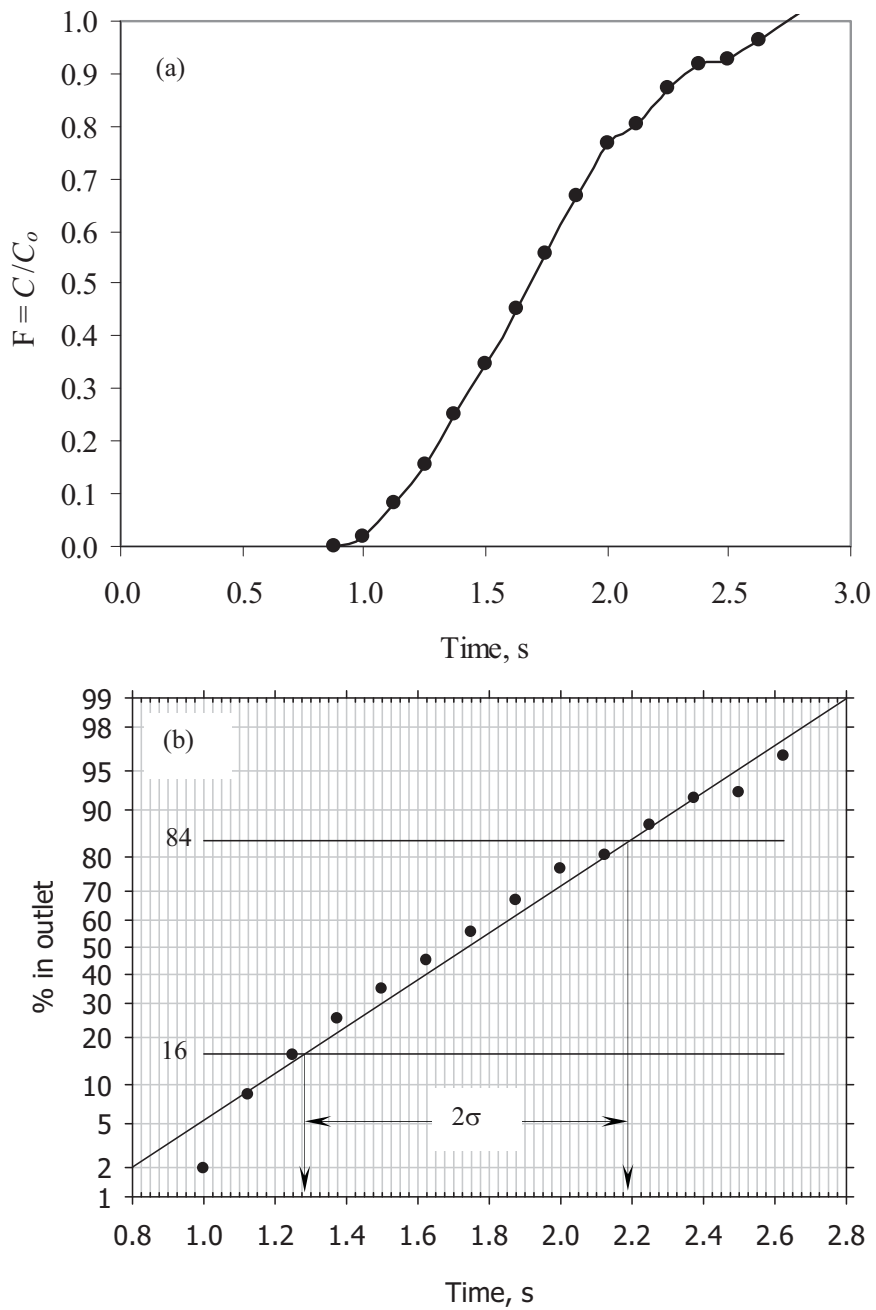


Figure 4. Step response curve and probability plot of the response signal for 4 alternating jets [adopted from Baawain et al. (2007)].

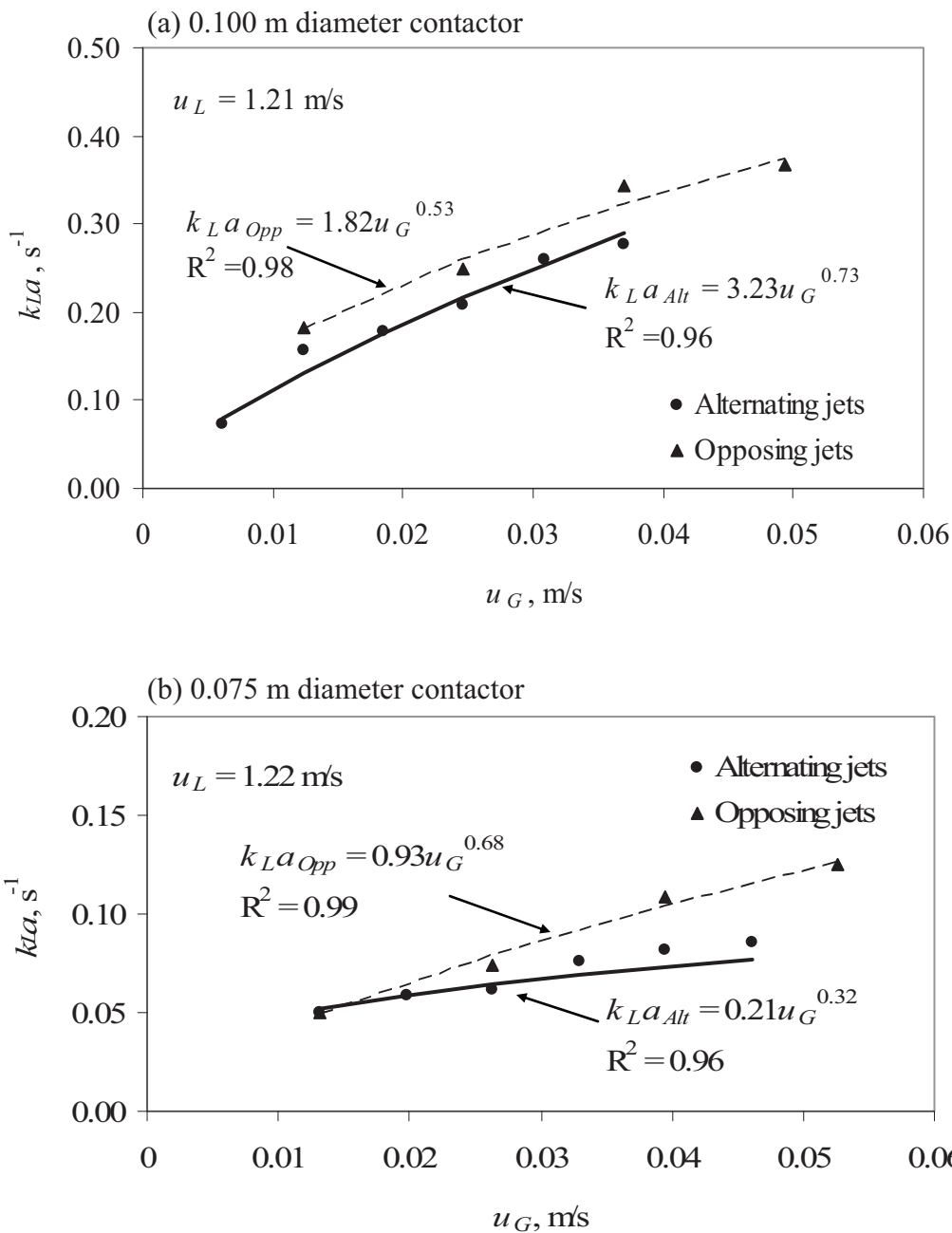


Figure 5. Overall mass transfer rate for alternating and opposing jets for the two ozone contactors.

Conclusions

This paper investigated the design of two pilot-scales of in-line multi-jets ozone contacting systems. A laser flow map particle image velocimetry coupled with a planar laser induced fluorescence (PIV/PLIF) were used to characterize the hydrodynamics of the contactors under different operating conditions. Velocity measurements of the two phases (liquid and gas), using the PIV system, were taken at different location along the contactors to evaluate the flow patterns within the two systems. The PLIF system was utilized to obtain the concentration distribution of a fluorescent dye at the end of the two contactors to examine the dispersion characteristics of the systems. A mass transfer study was also performed to determine the overall ozone mass transfer coefficient (k_{La-O_3}) under different operational conditions. Results obtained from both contactors indicated that the dispersion number increases as the number of two-phase jets increases. Furthermore, at the same number of jets, the dispersion number was higher when alternating jets were used. The k_{La-O_3} value was found to increase with the number of jets. Also, opposing jets configuration yielded higher k_{La-O_3} values compared alternating jets configuration. The larger ozone contactor showed higher k_{La-O_3} values compared to the smaller one.

Acknowledgements

The authors would like to acknowledge the financial support provided by Alberta Ingenuity, Mazzei[®] Injector Corp and the Ministry of Higher Education, Sultanate of Oman. The technical support provided by the technical staff at the University of Alberta is greatly appreciated.

References

1. Albrecht, H.E., M. Borys, N. Damaschke, and C. Tropea, *Laser Doppler and Phase Doppler Measurement Techniques*. (N. Y: Springer-Verlag Berlin Heidelberg, 2002).
2. Atkinson, J.F., J.V. Benschoten, and C.Y. Cheng, *Development of Particle Image Technology for Water Treatment Studies*. (Denver: AWWA Research Foundation, U.S.A., 2000).
3. Baawain, M.S., M. Gamal El-Din, D.W. Smith, and A. Mazzei "Hydrodynamic Characterization of an in-Line Opposing-Jets Ozone Contactor", *In Proc. of World Congress on Ozone and Ultraviolet Technologies (IOA/IUVA 2007)*, Los Angeles, CA USA, 10 p. (August 27-29, 2007).
4. Bernard, P.S., and J.M. Wallace, *Turbulent Flow: Analysis, Measurement and Prediction*. (Hoboken, N. J.: John Wiley & Sons, Inc., 2002).
5. Danckwerts P.V. *Gas-Liquid Reaction*. (N.Y.: McGraw-Hill, 1970).
6. Deckwer, W.-D., Burckhart, R., and Zoll, G. "Mixing and Mass Transfer in Tall Bubble Columns". *Chem. Eng. Sci.* 29, 2177-2188 (1974).
7. Durst, F., G. Brenn, and T.H. Xu, "A Review of the Development and Characteristics of Planar Phase-Doppler Anemometry", *Meas. Sci. Technol.*, 8: 1203-1221 (1997).
8. Joshi, J.B., "Reduction of Empiricism through Flow Visualization and Computational Fluid Dynamics", *Chem. Eng. Technol.*, 25(3): 321-328 (2002).

9. Joshi, J.B., and V.V. Ranade, " Computational Fluid Dynamics for Designing Process Equipment: Expectations, Current Status, and Path Forward", *Ind. Eng. Chem. Res.*, 42: 1115-1128 (2003).
10. Levenspiel, O., *Chemical Reaction Engineering*. (Hoboken, NJ.: J. Wiley & Sons, Inc., 1999).
11. Petrovic, M., S. Gonzalez, and D. Barcelo, "Analysis and Removal of Emerging Contaminants in Wastewater and Drinking Water ", *TrAC-Trends Anal. Chem.* , 22(10): 685-696 (2003).
12. Raffel, M., C. Willert, and J. Kompenhans, *Particle Image Velocimetry: A Practical Guide* . . (N. Y.: Springer-Verlag Berlin Heidelberg, 1998).
13. Roustan M, Wang RY, and Wolbert D. "Modelling Hydrodynamics and Mass Transfer Parameters in a Continuous Ozone Bubble Column". *Ozone Sci. & Eng.*, 18(2): 99-115 (1996).
14. Sherwood TK, Robert LP, Charles RW. *Mass Transfer*. (N.Y.: McGraw-Hill, 1975).